

Numerical analysis of a divergent duct with high enthalpy transonic cross injection

S. Ramechecandane^{1,*}, C. Balaji[†] and S. P. Venkateshan[‡]

^{*}Senior Software Developer, WindSim AS, 3115 Tonsberg, Norway¹

[†]Professor, Heat Transfer and Thermal Power Laboratory,
Department of Mechanical Engineering, Indian Institute of Technology
Madras, Chennai- 600 036, India.

[‡]Professor, Heat Transfer and Thermal Power Laboratory,
Department of Mechanical Engineering, Indian Institute of Technology
Madras, Chennai- 600 036, India.

ABSTRACT

In the present study, an aerothermodynamic analysis of high-speed flow fields through a divergent duct (similar to a supersonic combustor: hereafter referred to as supersonic combustor in the paper), without injection and with high enthalpy cross injection, has been performed. Initially, the thermal and flow analyses of the combustor are carried out by passing vitiated air at a temperature of 607.5 K, and this is followed by a computational analysis of the interaction of the flow field with the structure, when high enthalpy air is injected. The flow is turbulent in the combustor and the $k-\omega$ model has been considered to be appropriate for such cases, as it can resolve vorticity and highly strained flows. The study also emphasizes on the advantages of two-dimensional modelling over three dimensional modelling for cold flow cases in supersonic combustors, which could serve as an alternative, for wind tunnel tests as well as computationally expensive three dimensional numerical analysis. A comparison of various turbulence models for supersonic flows without cross injection has been carried out to arrive at the suitable model. For the cases of cross/transverse injection, the Mach numbers considered for investigation are 2, 2.5 and 3. The pressure, temperature and heat flux predictions for the cases with and without injection compare well with the experimental results.

Keywords: finite volume method, $k-\omega$ model, supersonic flows, flow field structural interaction, transverse injection.

1. INTRODUCTION

In the past few decades of hypersonic research, though adequate attention has been bestowed on fluid structural thermal interaction of external high-speed flows, not many studies have looked at fluid structural interaction in internal high-speed flows. The investigation of an inviscid compressible flow through a convergent divergent nozzle itself was difficult during the 1970s [1]. It was realized that quasi one-dimensional approximation cannot be relied

¹Email id: ramesh@windsim.com, Telephone: 004795446874

upon when the flow happens to be genuinely multi-dimensional. Earlier computational facilities and algorithms were incapable of producing results for complex, viscous, compressible, turbulent multi-dimensional flows. With the advent in current day high capacity computers, the solution of complex high-speed internal flows could be sought with much ease and less investment. More recently, many researchers have numerically investigated a number of high-speed flow problems (excluding structural interactions), notable being the investigation of non stationary compressible flows through convergent ducts with varying cross section by Igra et al. [2]. The study of the interaction of shock waves and boundary layer due to compressible flows through ducts has remained a challenging task even though much work has been done on this [2–8].

The advancement of the frontiers of hypersonic reentry vehicles and hypersonic air breathing engines has forced researchers to pay attention towards internal high-speed flows. The first phase of any supersonic combustor/DMR experiment would be to carry out a cold flow analysis using the physical model, notable being the scramjet engine tests carried out at National Aerospace Laboratory in Japan [3–5] and [10–11]. Analysis of fuel mixing in supersonic combustors has been carried out by some researchers [7–8]. The objective of the present study is to carry out a numerical investigation of high-speed flow fields through the supersonic combustor without fuel injection but with high enthalpy air injection, following the combined experimental and numerical work of Reinartz and Koschel [9].

2. MODELING

The supersonic combustor considered for investigation is made of Nimonic C-263 alloy, which finds its application widely in aerospace applications. The wall is of uniform thickness and of the same material throughout. The wall is 16 mm thick and is not cooled during the experiment [9]. The geometry considered for analysis is the same as considered by Reinartz and Koschel [9] and is shown schematically in Fig. 1. The model of the combustor has a constant area portion of 0.3 m and thereafter a divergent portion with a divergence angle of 2° , extending to 0.5 m. Following the divergent portion a constant area portion of 1.0 m is attached. Reinartz and Koschel have conducted experiments on a model of the supersonic combustor under controlled environment and have compared, the experimental results obtained with their numerical results (using the Finite Element Method). The tests were

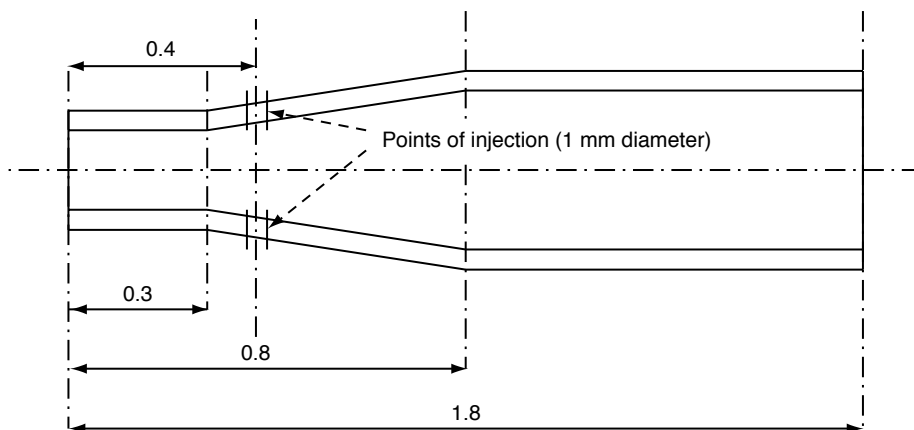


Figure 1 Schematic diagram of the supersonic combustor. (Figure not to scale, all indicated dimensions are in m)

conducted with injection as well as without injection. The test results for the case without injection serve as a validation. As the geometry is symmetric about the axis, the numerical analysis of one half is sufficient to obtain the parameters of interest.

2.1. OPERATING CONDITIONS INVESTIGATED

The inlet flow conditions of the test case [9] without injection are: Mach number – 3.0, total pressure – 2.33 MPa, total temperature-1701 K and mass flow rate – 1.6 kg/s. The injection of hydrogen is simulated by injecting a cold air jet at a Mach number of 1.05 and a stagnation or total pressure of 1.6 MPa. The static temperature of injection is taken to be 280 K. In the present study, three cases have been investigated for flow with cross/transverse injection of air at Mach numbers of 2.0, 2.5 and 3.0. For each case, the temperature of air at the inlet has been taken as 607.5 K [9]. The operating pressure has been taken as atmospheric. The stagnation pressure and temperature are obtained using isentropic relations given by (1) and (2).

$$\frac{T_o}{T_\infty} = 1 + \frac{\gamma - 1}{2} M^2 \quad (1)$$

$$\frac{p_o}{p_\infty} = \left(1 + \frac{\gamma - 1}{2} M^2 \right)^{\frac{\gamma}{\gamma - 1}} \quad (2)$$

The Reynolds number, speed of sound, Mach number and hydraulic diameter are given by (3)

$$\text{Re} = \frac{VD_h}{\nu}, a = \sqrt{\gamma RT}, M = \frac{V}{a} \text{ and } D_h = \frac{4A}{P} \quad (3)$$

Since the combustor is a divergent one the hydraulic diameter D_h varies along its length.

2.2. COMPUTATIONAL DOMAIN

The geometry is not complex and so a structured mesh would suffice and this is generated with the help of a gridding software [13]. The size of the mesh near the wall has to be fine enough to resolve the viscous sub layer. The number of cells generated is more than the number of cells considered in [9].

2.3. THERMO-PHYSICAL PROPERTIES

The density and specific heat capacity of Nimonic C-263 alloy have been considered as constant. However the thermal conductivity is given as a function of temperature and the values that are input to the code are listed below:

Density $\rho = 7950 \text{ kg/m}^3$.

Specific heat $C_p = 500 \text{ J/kg K}$.

Thermal conductivity $k = 11.42 + 0.0158 T + 10^{-6} T^2$.

Air is considered to be thermally perfect and hence the density follows ideal gas equation. The thermal conductivity and specific heat were assumed to follow kinetic theory of gases and the dynamic viscosity of air is obtained from Sutherland's empirical equation [9].

2.4. BOUNDARY CONDITIONS

The pressure inlet condition is specified at the entry of the combustor and the temperature at the inlet is taken as 607.5 K. Pressure outlet is specified as the boundary condition at the outlet. Adiabatic condition is imposed at the outer wall. The duct is symmetric about the mid plane and hence the solution to one half would be similar to the other half. Hence, symmetry boundary condition is imposed at the horizontal symmetry plane. The walls establishing contact with the fluid are coupled and hence coupled wall boundary condition is imposed for the inner walls of the combustor. The schematic of the geometry considered for investigation along with the boundary conditions imposed is shown in Fig. 2. A turbulence intensity of 2.8% has been considered for the present investigation following [9].

2.5. NUMERICAL MODELING

The solver used is a coupled implicit solver with second order unsteady formulation. The convergence criterion set for mass and momentum residuals is 10^{-3} , and for energy the residuals is 10^{-6} . The upwinding is of second order and Menter's $k-\omega$ turbulence closure has been employed. The Shear Stress Transport (SST) $k-\omega$ model or the Menter's $k-\omega$ model solves the standard $k-\omega$ model in the inner region of the boundary layer and a high-Reynolds-number version of the $k-\epsilon$ model in the outer part of the boundary layer. The Menter's $k-\omega$ model includes a modified turbulent viscosity formulation to account for the transport effects of the principal turbulent shear stress [12].

Using Reynolds averaging, the continuity and momentum equations in Cartesian coordinates turn out to be

$$\frac{\partial \rho}{\partial t} + \frac{\partial}{\partial x_i}(\rho u_i) = 0 \quad (6)$$

$$\frac{\partial}{\partial t}(\rho u_i) + \frac{\partial}{\partial x_j}(\rho u_i u_j) = -\frac{\partial p}{\partial x_i} + \frac{\partial}{\partial x_j} \left[\mu \left(\frac{\partial u_i}{\partial x_j} + \frac{\partial u_j}{\partial x_i} - \frac{2}{3} \delta_{ij} \frac{\partial u_l}{\partial x_l} \right) \right] + \frac{\partial}{\partial x_j}(-\rho u_i' u_j') \quad (7)$$

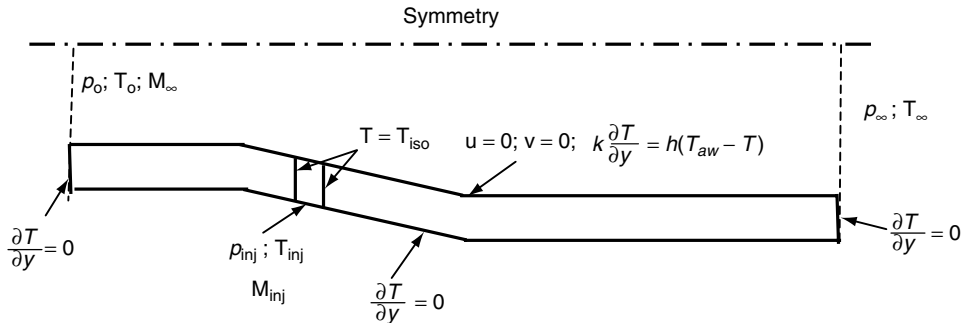


Figure 2 Boundary conditions. (not to scale)

The Reynolds stresses $\rho u'_i u'_j$ in the eqn. 7 must be modeled in order to close the equation. A common method employs the Boussinesq hypothesis to relate the Reynolds stresses to the mean velocity gradients (8).

$$-\overline{\rho u'_i u'_j} = \mu_t \left(\frac{\partial u_i}{\partial x_j} + \frac{\partial u_j}{\partial x_i} \right) - \frac{2}{3} \left(\rho k + \mu_t \frac{\partial u_i}{\partial x_i} \right) \delta_{ij} \quad (8)$$

The Boussinesq hypothesis is used in the Spalart-Allmaras model, the k - ε models, and the k - ω models. The advantage of this approach is the relatively low computational cost associated with the computation of the turbulent viscosity (μ_t). In the case of the Spalart-Allmaras model, only one additional transport equation (representing turbulent viscosity) is solved. In the case of the k - ε and k - ω models, two additional transport equations (for the turbulence kinetic energy, k , and either the turbulence dissipation rate, ε , or the specific dissipation rate (ω) are solved, and μ_t is computed as a function of k and ε or ω . The disadvantage of the Boussinesq hypothesis as presented is that it assumes μ_t is an isotropic scalar quantity, which is not strictly true. In addition to the Reynolds averaged Navier Stokes equations and the energy equation, there are two additional equations for turbulent kinetic energy and specific dissipation rate. The tensorial form of the equations is as given in equations (9) and (10).

$$\frac{\partial}{\partial t}(\rho k) + \frac{\partial}{\partial x_i}(\rho k u_i) = \frac{\partial}{\partial x_j} \left(\Gamma_k \frac{\partial k}{\partial x_j} \right) + G_k - Y_k + S_k \quad (9)$$

$$\frac{\partial}{\partial t}(\rho \omega) + \frac{\partial}{\partial x_i}(\rho \omega u_i) = \frac{\partial}{\partial x_j} \left(\Gamma_\omega \frac{\partial \omega}{\partial x_j} \right) + G_\omega - Y_\omega + S_\omega + D_\omega \quad (10)$$

The effective diffusivities for the SST k - ω model are given by equations (11) and (12)

$$\Gamma_k = \mu + \frac{\mu_t}{\sigma_k} \quad (11)$$

$$\Gamma_\omega = \mu + \frac{\mu_t}{\sigma_\omega} \quad (12)$$

Where σ_k and σ_ω are the turbulent Prandtl numbers for k and ω , respectively. The turbulent viscosity, μ_t , is computed using equation (13) and the turbulent Prandtl numbers by equations (15) and (16)

$$\mu_t = \frac{\rho k}{\omega} \frac{1}{\max \left[\frac{1}{\alpha^*}, \frac{\Omega F_2}{\alpha_1 \omega} \right]} \quad (13)$$

$$\Omega = \sqrt{2\Omega_{ij}\Omega_{ji}} \quad (14)$$

$$\sigma_k = \frac{1}{\frac{F_1}{\sigma_{k,1}} + \frac{(1-F_1)}{\sigma_{k,2}}} \quad (15)$$

$$\sigma_k = \frac{1}{\frac{F_1}{\sigma_{\omega,1}} + \frac{(1-F_1)}{\sigma_{\omega,2}}} \quad (16)$$

A detailed explanation about blending functions F_1 and F_2 and the production and dissipation of turbulent kinetic energy and specific dissipation rate is available in [12].

The model constants are given the values as mentioned below

$$\sigma_{k,1} = 1.176 \quad \sigma_{\omega,1} = 2.0 \quad \sigma_{k,2} = 1.0 \quad \sigma_{\omega,2} = 1.168$$

The default values of model constants and turbulence viscosity in the solver was used for the present investigation. A detailed explanation of the Menter's k- ω model is given in [12].

3. RESULTS AND DISCUSSION

All cases considered for investigation are solved using unsteady coupled implicit solver with second order formulation. It is a common practice to validate the codes generated for turbulent compressible flows with some standard benchmark cases. However, since the software employed in this study has been well tested, we propose to directly compare the predictions with experimental results obtained, for the geometry considered. In the present study, the experimental results by Reinartz and Koschel [9] for supersonic flows through the model of the supersonic combustor (without injection), have been considered as a source for validation. The first phase of any NUMERICAL analysis would be to carry out a grid dependence/independence study to decide upon whether solution is grid independent or not. Unlike three dimensional NUMERICAL analysis, as the geometry considered is two-dimensional the grid independence could be carried out by associating the number of grids with different flow and heat transfer parameters/variables. In the case of supersonic flows without cross injection the grid independence is carried out with 35,000 cells, 50,000 cells and 70,000 cells. The wall temperature distribution along the length of the combustor reveals that there exists less than 1% variation between the 50,000 and 70,000 cells cases. However, to be more conservative, 70,000 cells have been considered as the optimum number of cells for all investigations.

The wall temperature distribution along the combustor showed that the temperature is a maximum at the entry region and thereafter decreases gradually and reaches a minimum at the exit. The oscillation of temperature near the divergent section reveals that shock interaction is considerable there as the geometry undergoes a sudden expansion. The expansion wave makes the flow parameters to oscillate spatially. Hence, the measurement of such flows must be carried out at a number of points along the combustor [9]. The numerical investigation carried out compared well with the experimental results. The pressure

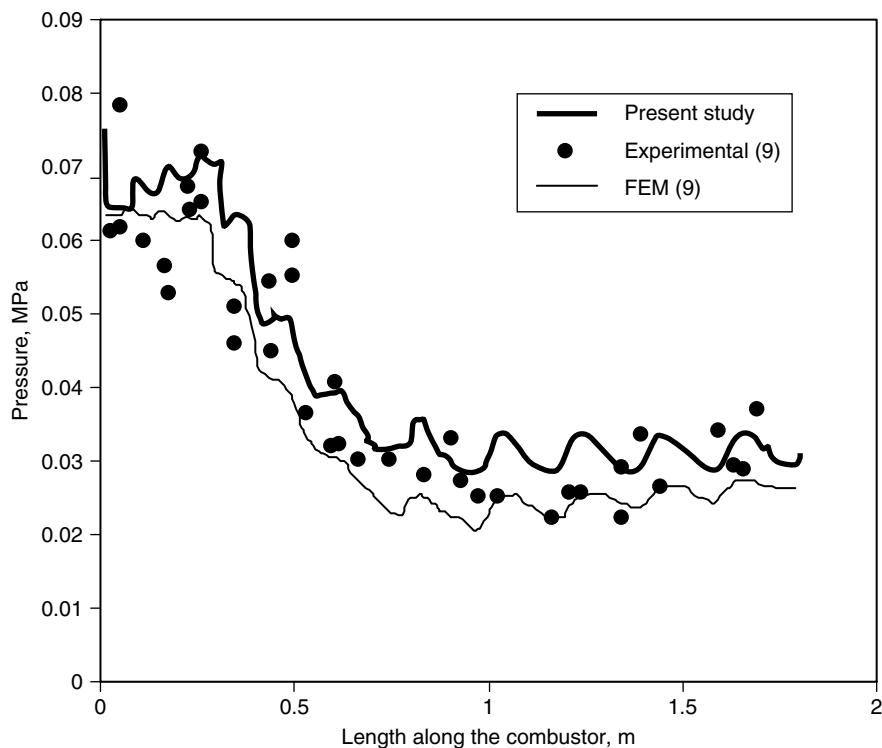


Figure 3 Distribution of static pressure along the combustor length. (without injection)

distribution at the coupled wall (Fig. 3) shows that the pressure is a maximum at the entry to the constant area section and thereafter decreases gradually along the divergent section and once again stabilizes along the constant cross sectional area - outlet section. The pressure distribution estimated through the numerical investigation deviates from 5 kPa to a maximum of 10 kPa from the mean of the experimental values.

The pressure plot of Fig. 3 also shows that the experimental values themselves exhibit oscillations and it is quite difficult to arrive at a single value of pressure at a fixed location. The finite element method used by Reinartz and Koschel [9] shows close agreement to their experimental measurements. The prediction of pressure by the present study shows that though it predicts the peak values measured by experiments, it shows a bit of deviation from the clustered values of experimental measurements. Figure 3 seems to lead to the conclusion that the finite element predictions by Reinartz and Koschel [9] and the present calculations are equally good.

In the past, adequate attention has been paid to supersonic injection with relevance to supersonic combustion and most of available literature discusses the effect of supersonic cross/transverse injection including combustion. The objective of the present study is to bring out the effects of supersonic cross injection on a main stream of supersonic flow. In view of this, high enthalpy air is injected into the supersonic air stream thereby obviating the need to consider chemical reactions associated with combustion.

The Mach number contours of Fig. 4 show that for Mach 3.0 inlet flow conditions three upstream vortices are formed because of high pressure main flow as well as high pressure

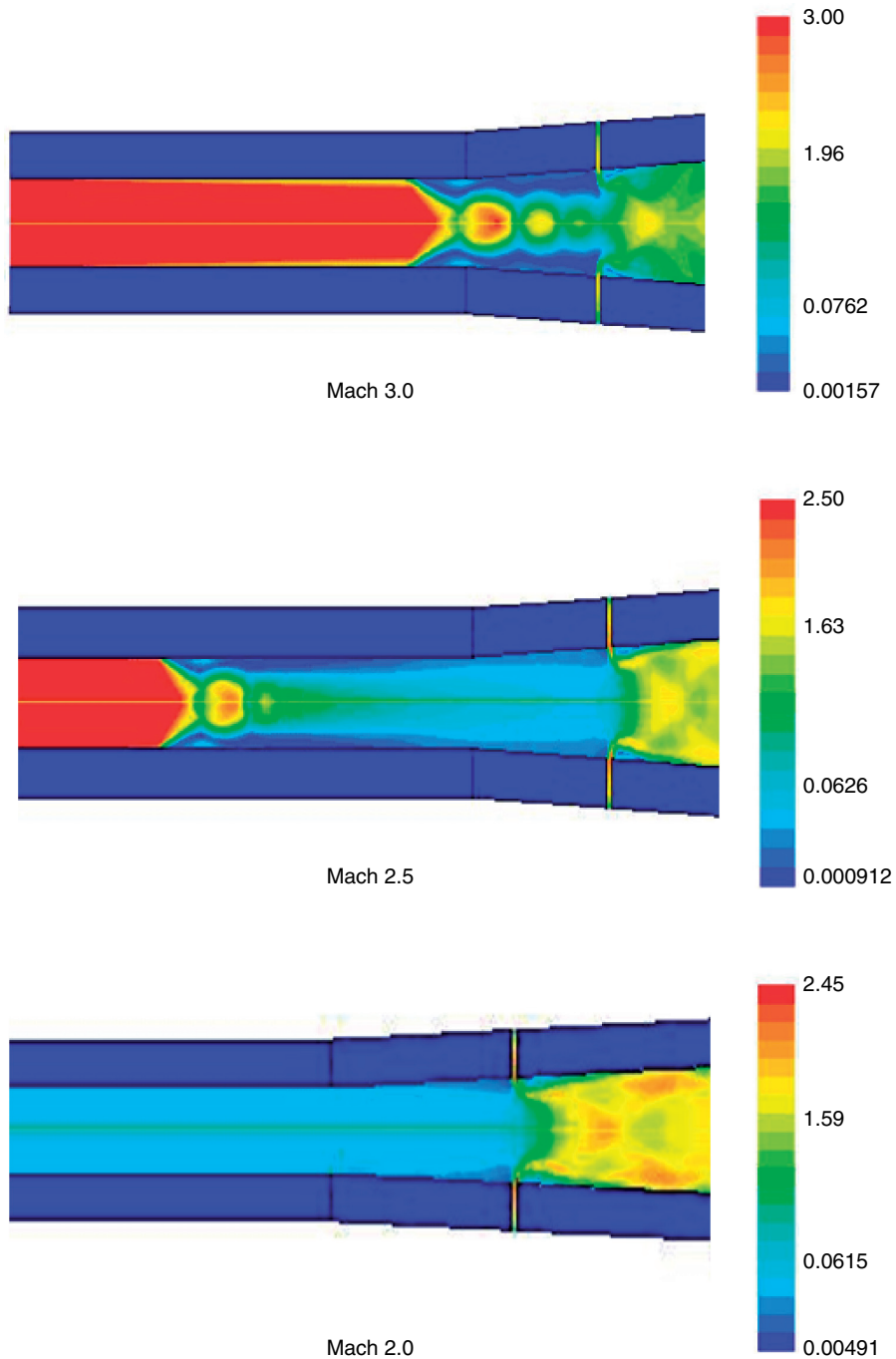


Figure 4 Mach number contour plot of the injection area mirrored along the symmetry line.

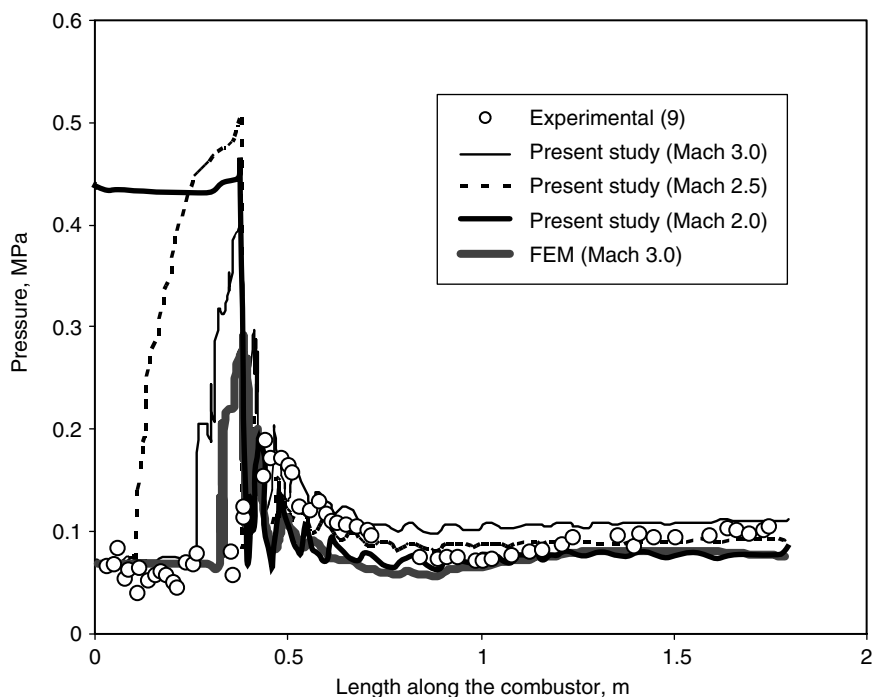


Figure 5 Distribution of wall pressure along the combustor length for various Mach numbers.

cross injection. In the case of Mach 2.5, two vortices are formed due to cross injection. The pressure of injection is much higher than the pressure of the main flow stream for Mach 2.0 condition and hence the flow upstream is relatively reduced at a low Mach number because of cross injection. No vortex formation is seen to occur.

The distribution of wall pressure for different Mach numbers is shown in Fig. 5. The pressure distribution near the entrance shows variation with respect to the main stream Mach number. The pressure peaks are mainly because of cross injection. The shock/shock interaction and the boundary layer interaction might also be held responsible for an unpredictable behavior of pressure at the regions near the divergent portions.

The heat flux distribution along the combustor in Fig. 6 shows that the heat flux decreases along the combustor in the constant area section and suddenly shows two peaks due to a pressure rise at the points of injection. At the point of injection the temperature of cross injected air is low and because of that the heat flux falls to a minimum.

The heat flux gradually increases after the point of injection. This shows that the heat flux is totally dependent on the pressure rather than the temperature after the points of cross injection. The distribution of wall heat flux by FEM analysis shows the occurrence of two peaks corresponding to the point of injection and then falls to almost zero like the predictions obtained in this study. The major contributor of heat flux is the pressure of main stream and cross injection and not the temperature.

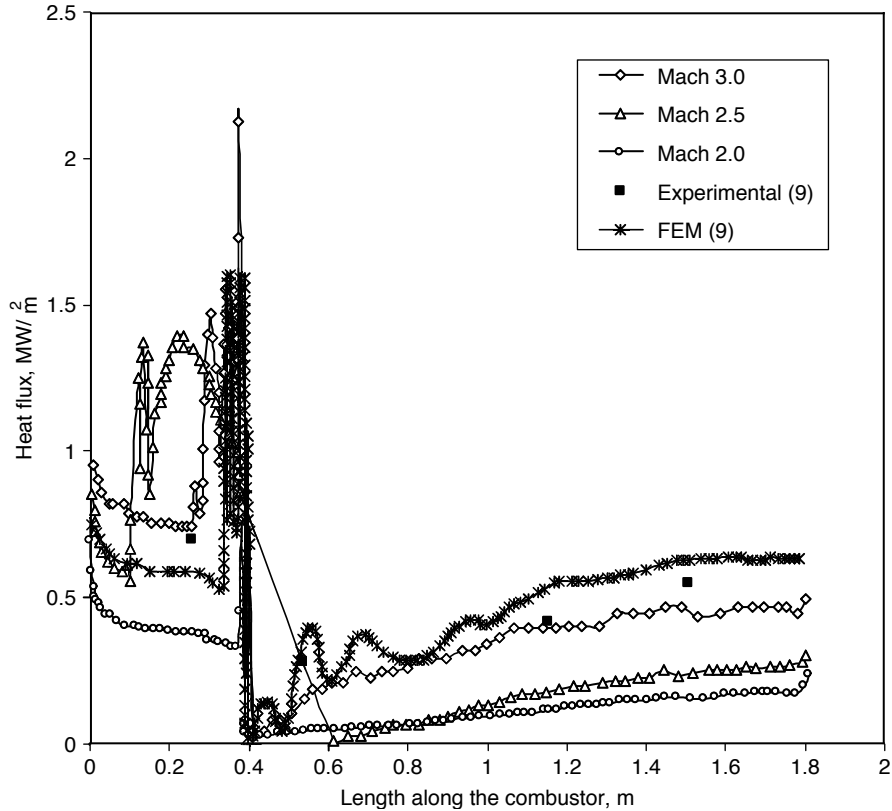


Figure 6 Distribution of wall heat flux along the combustor length in comparison to the experimental results for Mach 3.0 [9].

4. CONCLUSIONS

A numerical investigation of high-speed internal flows with supersonic cross/transverse injection has been carried out on a SGI origin compute server. The study clearly brings out the adequacy of a two-dimensional numerical analysis which was found to give fair agreement with experimental results. Hence, the two-dimensional numerical analysis could serve as an effective substitute for power consuming wind tunnel tests. An analysis of the fluid structural interaction for supersonic cross flows shows that the heat flux predictions are in good agreement with experimental results and, hence, it is possible to obtain the values of heat flux at points wherein experimental measurement is impossible or quite difficult. The use of Menter's $k-\omega$ turbulence model yields reliable results for such high-speed internal flows with supersonic cross injection. For the geometry under consideration, the pressure of the mainstream air as well as the cross-injection contributes significantly to the rise in the heat flux in comparison to the temperature.

REFERENCES

- [1] Anderson, J. D., *Computational Fluid Dynamics*, McGraw-Hill, New York, 1997.
- [2] Igra, L. W., Falcovitz, J., "Non Stationary Compressible Flow in Ducts with Varying Cross-Section", *IMEchE*, vol. 212, 1998, pp. 225–243.

- [3] Mitani. T., Kanda. T., Hiraiwa. T., Tomioka. S., Chinzei. N., “Mach 6 Testing of a Scramjet Engine Model”, *Journal of Propulsion and Power*, vol. 13, 1997, pp. 543–551.
- [4] Mitani. T., Kanda. T., Hiraiwa. T., Igarashi. Y., Kazuhiro. N., “Drags in Scramjet Engine Testing: Experimental and Computational Fluid Dynamics Studies”, *Journal of Propulsion and Power*, vol. 15, 1999, pp. 578–583.
- [5] Mitani. T., Kanda. T., Tomioka. S., Tani. K., and Sunami. T., “Mach 6 Testing of a Scramjet Engine Model”, *Journal of Propulsion and Power*, vol.17, 2001, pp. 132–138.
- [6] Drummond. J. P., Diskin. G. S., Cutler. J. D., “Fuel-Air Mixing and Combustion in Scramjets”, *AIAA*, 2002, pp. 3878.
- [7] Northam. G. B., Capriotti. D. P., “Evaluation of Parallel Injector Configurations for Mach 2 Configuration”, *Journal of Propulsion and Power*, vol. 8, 1992, pp. 491–499.
- [8] Claus. R. W., Vanka. S. P., “Multigrid Calculations of a Jet in Cross Flow”, *Journal of Propulsion and Power*, vol. 8, 1992, pp. 425–431.
- [9] Reinartz. B. U., Koschel. W. W., “Thermal Analysis of Fluid – Structural Interaction in High – Speed Engine Flowfields”, *Journal of Propulsion and Power*, vol. 17, 2001, pp. 1339–1346.
- [10] Von Lavante. E., Zeitz. D., Kallenberg. M., “Numerical Simulation of Supersonic Airflow with Transverse Hydrogen Injection”, *Journal of Propulsion and Power*, vol. 17, 2001, pp. 1319–1327.
- [11] Burton Northam. G., Capriotti. D. P., “Evaluation of Parallel Injector Configurations for Mach 2 Combustion”, *Journal of Propulsion and Power*, vol. 8, 1992, pp. 491–499.
- [12] FLUENT 6.2 user’s guide. Fluent Inc., USA, 2005.
- [13] GAMBIT 6.2 user’s guide. Fluent Inc., USA, 2005.

LIST OF SYMBOLS

a	velocity of sound (m/s)
A	cross sectional area (m ²)
D_h	hydraulic diameter (m)
G	generation term
K	turbulent kinetic energy (m ² /s ²)
P	perimeter (m)
p	pressure (N/m ²)
R	gas constant (J/kg K)
S	source term
Re	Reynolds number
M	Mach number
T	temperature (K)
V	velocity of flow (m/s)
Y	dissipation term

Greek Symbols

γ	ratio of specific heats
ν	kinematic viscosity (m ² /s)
ω	specific dissipation rate (1/s)
Γ	effective diffusivity (m ² /s)
σ	turbulent Prandtl Number

Subscripts

o	stagnation condition
∞	main stream condition

iso	isothermal condition
K	turbulent kinetic energy
ω	specific dissipation rate

Acronyms

NUMERICAL	Computational Fluid Dynamics
DMR	Dual Mode Ram Jet
FEM	Finite Element Method